scientific reports

Check for updates

OPEN

Comparison of ^{68}Ga-DOTATATE and ^{18}F-FDG PET/CT for tumor staging and primary tumor volume delineation in patients with nasopharyngeal carcinoma

Haoyuan Ding[1,2,3,6], Juan Liang[4,6], Yudi Wang[1,2,3], Kaixiang He[5], Lin Liu[1,2,3], Ya Liu[1,2,3,7]✉ & Yue Chen[1,2,3,7]✉

This study evaluated the clinical utility of ^{68}Ga-DOTATATE PET/CT compared to ^{18}F-FDG PET/CT for tumor staging and the delineation of primary tumor volume in patients with non-keratinizing nasopharyngeal carcinoma (NPC). Forty-two individuals with pathologically confirmed non-keratinizing NPC were recruited. This study compared the detection rates of primary and metastatic tumors and the accuracy of tumor staging using two PET/CT modalities. Tumor volumes defined on PET scans using the absolute SUV of 2.5 (TH2.5), 40% of the maximum SUV (TH40%), and the relative background-dependent threshold (THbgd) were analyzed in comparison to MRI results. Comparing ^{68}Ga-DOTATATE and ^{18}F-FDG PET/CT, identifying primary tumors (initial detection, 100% vs. 97.3%; recurrent detection, 80.0% vs. 100%) and lymph node metastases (99.0% vs. 100%) were comparable. However, ^{68}Ga-DOTATATE PET/CT detected more skull base bone (100% vs. 96.3%) and intracranial invasion (100% vs. 54.5%) than ^{18}F-FDG, and consequently correctly upwardly adjusted the T-staging in 7 patients. ^{68}Ga-DOTATATE PET/CT detected an equal number of lung metastases (24/24) but more bone metastases (97.8% vs. 84.4%) compared to ^{18}F-FDG PET/CT, yet was less effective for liver metastases (30.4% vs. 100%). Compared with ^{18}F-FDG PET/CT, ^{68}Ga-DOTATATE PET/CT correctly upstaged 5 subjects and downstaged 1 subject in overall staging. Tumor volumes assessed by ^{68}Ga-DOTATATE PET compared to ^{18}F-FDG PET using the three threshold methods demonstrated less variability and higher agreement with MRI. Among the methods, THbgd for lesion segmentation in ^{68}Ga-DOTATATE PET demonstrated the highest confidence level and concordance with MRI (ICC 0.95). In conclusion, ^{68}Ga-DOTATATE PET/CT is a beneficial complement to ^{18}F-FDG PET/CT for NPC staging, with higher accuracy for primary tumor volume delineation.

Keywords ^{18}F-FDG, ^{68}Ga-DOTATATE, Nasopharyngeal cancer, PET/CT

Nasopharyngeal carcinoma (NPC) is the most prevalent epithelial malignancy in the area of the head and neck[1]. While NPC is relatively uncommon, it displays significant prevalence in particular regions, particularly East and Southeast Asia[2]. The insidious onset of NPC and its propensity for early metastasis result in many patients receiving diagnoses at advanced stages of the disease. The clinical stage of NPC significantly influences prognosis. Upon reaching an advanced stage, the patient's mortality rate is increased considerably[3]. Therefore, early identification and accurate staging are essential to diagnosing and treating patients with NPC.

[1]Department of Nuclear Medicine, The Affiliated Hospital of Southwest Medical University, No. 25 Taiping St, Jiangyang District, Luzhou 646000, Sichuan, People's Republic of China. [2]Nuclear Medicine and Molecular Imaging Key Laboratory of Sichuan Province, Luzhou 646000, Sichuan, People's Republic of China. [3]Institute of Nuclear Medicine, Southwest Medical University, No. 25 Taiping St, Jiangyang District, Luzhou 646000, Sichuan, People's Republic of China. [4]Department of Ultrasound, The Affiliated Hospital of Southwest Medical University, No 25. Taiping St, Jiangyang District, Luzhou 646000, Sichuan, People's Republic of China. [5]Department of Oncology, The Affiliated Hospital of Southwest Medical University, No. 25 Taiping St, Jiangyang District, Luzhou 646000, Sichuan, People's Republic of China. [6]These authors contributed equally: Haoyuan Ding and Juan Liang. [7]These authors jointly supervised this work: Ya Liu and Yue Chen. ✉email: 1935221414@qq.com; chenyue5523@126.com

Integrating metabolic and anatomical data in ^{18}F-FDG PET/CT offers substantial advantages over anatomical imaging alone. In patients with NPC, it enhances the accuracy of staging and the evaluation of therapeutic response. The presence of inflammatory and reactive hyperplastic lymph nodes in the neck, combined with the inflammatory response induced by radiotherapy and chemotherapy, complicates the accurate detection of local residual or recurrent tumors and lymph node metastasis using ^{18}F-FDG PET/CT[4]. Radiation therapy is the primary therapeutic option for NPC. Target tumor volume depicted *via* ^{18}F-FDG PET/CT correlates with radiotherapy efficacy[5,6]. Moreover, the tumor volume delineated based on ^{18}F-FDG PET is highly dependent on the method used for PET signal segmentation, with different thresholds yielding different tumor volumes[7–10]. However, the lack of authoritative standardized uptake value (SUV) lesion segmentation methodologies considerably reduces the validity of tumor volumes determined by ^{18}F-FDG PET/CT.

In areas with high NPC prevalence, non-keratinizing squamous carcinoma with Epstein-Barr virus (EBV) infection has the highest frequency (> 95%)[1,11]. EBV infection significantly raises NPC tissue somatostatin receptor 2 (SSTR2) expression[12,13]. [^{68}Ga-DOTA, Tyr3]-octreotate (^{68}Ga-DOTATATE) PET/CT targeting SSTR2 detected primary and metastatic NPC tumors effectively previously reported studies[14,15]. An optimal tumor background ratio enhances the visualization of the primary tumor. Thresholding methods represent commonly used techniques for quantifying biological target volumes in PET imaging. To our knowledge, the use of ^{68}Ga-DOTATATE PET for assessing and defining primary tumor volumes in NPC has not been previously documented.

In this context, this study aimed to investigate further the efficacy of ^{68}Ga-DOTATATE PET/CT in identifying primary and metastatic NPC and to evaluate its influence on tumor staging compared to ^{18}F-FDG PET/CT. Moreover, focused segmentation was conducted employing various SUV threshold methodologies to assess the precision of primary tumor volume delineation using ^{68}Ga-DOTATATE PET.

Methods

Participant cohort and study design

This single-center prospective study investigated ^{68}Ga-DOTATATE PET/CT in non-keratinizing nasopharyngeal carcinoma. The Clinical Research Ethics Committee of the Affiliated Hospital of Southwest Medical University approved the study (Approval No. 2020035), adhering to the 1964 Declaration of Helsinki and its subsequent revisions. Every participant provided informed consent. Eligible patients were recruited at our facility from June 2022 to December 2022. In a week, all MR scanning, ^{68}Ga-DOTATATE PET/CT, and ^{18}F-FDG PET/CT were completed in this order, with no less than one day elapsed between the acquisitions of ^{68}Ga-DOTATATE PET/CT and ^{18}F-FDG PET/CT. The following criteria were applied to determine the study participants: (1) Patients with histopathologically proven non-keratinizing NPC who are either newly diagnosed or have previously had treatment; (2) Patients who have not received anti-tumor medication in the preceding three months. The exclusion criteria of the study were: (1) Patients with multiple primary malignant tumors; (2) Individuals for whom the examination was inappropriate.

^{18}F-FDG and ^{68}Ga-DOTATATE Preparation

Standard procedures were followed to synthesize ^{18}F-FDG using an ^{18}F-FDG-compliant synthesis module (FDG-N, PET Science & Technology). ^{68}Ga-DOTATATE was synthesized using established methodologies[16]. Radiochemical purities of both were greater than 95%.

Imaging acquisition

The individuals fasted for at least 6 h before the ^{18}F-FDG PET/CT to maintain normal blood glucose levels (3.9–6.1 mmol/L). The ^{68}Ga-DOTATATE PET/CT requires no specific preparation. ^{68}Ga-DOTATATE and ^{18}F-FDG were administered intravenously at concentrations of 1.85 MBq/kg and 3.7 MBq/kg, respectively. The PET/CT imaging was conducted sixty minutes post-radiotracer administration. Every scan followed a previously published technique[16,17], and a post-processing workstation (version R002, UWS-MI, United Imaging Medical) uploaded the collected data. The nasopharyngeal and neck contrast-enhanced MR exams were conducted using previously published techniques[17].

Imaging analysis

Two nuclear medicine physicians (L.Q and Z.H) and two radiologists (P.L and G.C) independently and randomly interpreted PET/CT and MRI images. Reviewers were unaware of additional imaging data. For primary tumors, visual assessment of boundaries was performed by comparing radiotracer uptake at lesion margins with adjacent healthy tissue on PET images. The boundaries and extent of lesion invasion were identified when radiotracer uptake at the margin was significantly higher than background values. Lesion morphology identification and localization were aided by co-registered CT. Each primary tumor's margins and extent were assessed, and any differences between MRI, ^{68}Ga-DOTATATE PET/CT, and ^{18}F-FDG PET/CT were documented. For metastatic tumors, lesions demonstrating radiotracer uptake above normal tissue background (with or without morphological abnormalities) were defined as positive after excluding physiological uptake and benign lesions on PET/CT. As per the 9th edition of the American Joint Committee on Cancer staging system, the clinical staging was determined based on ^{68}Ga-DOTATATE PET/CT and ^{18}F-FDG imaging methods[18], respectively.

The diagnosis was confirmed by the lesion's histopathology. For evaluating initial tumor infiltration, contrast-enhanced MRI was the gold standard[19]. Follow-up was acquired for metastatic lesions with unobtainable pathohistologic results. According to the RECIST 1.1 recommendations[20], during follow-up, a lesion was considered malignant if multiple imaging examinations demonstrated classic signs of malignancy, and there was a significant increase (≥ 20% in longest diameter) or decrease (≥ 30% in longest diameter) in target lesion size following anti-tumor therapy.

Characteristics	Number
No. patients	42
Age (year)	
Mean ± standard deviation	49 ± 11
Gender	
Male	33
Female	9
Histology, WHO type	
Diferentiated non-keratinizing carcinomas	19
Undiferentiated non-keratinizing carcinomas	23
Patient status	
Initial assessment	37
Recurrence or metastasis detection	5

Table 1. Patient characteristics.

Site of disease	No. of patients	No. of lesions	^{18}F-FDG uptake			^{68}Ga-DOTATATE uptake			*P* value (SUVmax)	*P* value (lesions detection)
			SUVmax	No. of Positive Lesions	Detection rates (%)	SUVmax	No. of Positive Lesions	Detection rates		
Primary tumors	37	37	15.83 ± 8.31	36	97.3	8.79 ± 3.84	37	100%	< 0.001	*N*
Local recurrence	5	5	11.7* (7.7–26.7)	5	100	7.4* (5.0-10.5)	4	80%	*N*	*N*
Lymph nodes	36	202	9.6 ± 7.05	202	100	6.0 ± 4.17	200	99.0%	< 0.001	0.05
Distant metastases										
Liver	3	23	4.7* (3.4–25.5)	23	100	10.0* (8.4–10.8)	7	30.4%	0.02	<0.001
Lung	2	24	3.95* (1.4–25.9)	24	100	1.65* (0.9–5.3)	24	100%	< 0.001	*N*
Bone	5	45	11.1 ± 10.02	38	84.4	6.33 ± 3.74	44	97.8	< 0.001	0.07

Table 2. Comparison of semi-quantitative parameters and lesions detection between ^{18}F-FDG and ^{68}Ga-DOTATATE PET/CT. Data were presented as mean ± standard deviation. *median, *N* = not application.

Tumor volume delineation

The parameters were determined automatically after Hermes software identified tumor areas of interest on PET/CT and MR images. To determine the primary tumor volume on MRI, an area of interest was manually identified layer by layer along the lesion edge using enhanced T1WI images. The threshold techniques used to assess ^{18}F-FDG and ^{68}Ga-DOTATATE primary tumor volumes were[21]: (1) The SUV absolute threshold of 2.5 (TH2.5); (2) The SUV relative threshold of 40% of SUVmax (TH40%); (3) The relative background dependent threshold (THbgd). THbgd was calculated as SUV = SUVbgd + 20% (SUVmax - SUVbgd), where SUVbgd is the mean SUVmax of 10 randomly defined regions of interest in the non-pathological area surrounding the primary tumor, excluding the brain, salivary glands, oral cavity, and orbital region. The contours delineating the volume of interest are established on the PET image using the specified thresholds, and the contours surrounding the target lesion inside the defined boundary are automatically produced to compute the tumor volume.

Statistical analyses

The statistical analysis was performed with SPSS 25.0 (IBM). The quantitative data were presented as the mean ± standard deviation (SD) or median. The sensitivity of the two radiotracers was compared using McNemar's test. The SUVmax of primary tumors and metastases was compared using ^{18}F-FDG and ^{68}Ga-DOTATATE PET/CT by the paired t-test and Mann-Whitney test. The intragroup correlation coefficient (ICC) was utilized to compare the consistency of the tumor volume between enhanced MRI and PET/CT at different thresholds. Two-tailed $p < 0.05$ indicated statistical significance.

Results

Patient characteristics

In the final stage, 42 participants were enrolled in the study, comprising 5 patients scheduled to have testing for metastasis or recurrence and 37 newly diagnosed patients. Participant characteristics are displayed in Table 1.

Comparison of ^{68}Ga-DOTATATE PET/CT versus ^{18}F-FDG PET/CT to assess the primary and metastatic lesions

Table 2 compares lesion detection and radiotracer uptake between the two modalities. ^{68}Ga-DOTATATE and ^{18}F-FDG PET/CT had comparable primary tumor detection rates. In one newly diagnosed patient, ^{18}F-FDG PET/CT and MRI were unable to identify the primary tumor (Fig. 1). One of the instances of primary

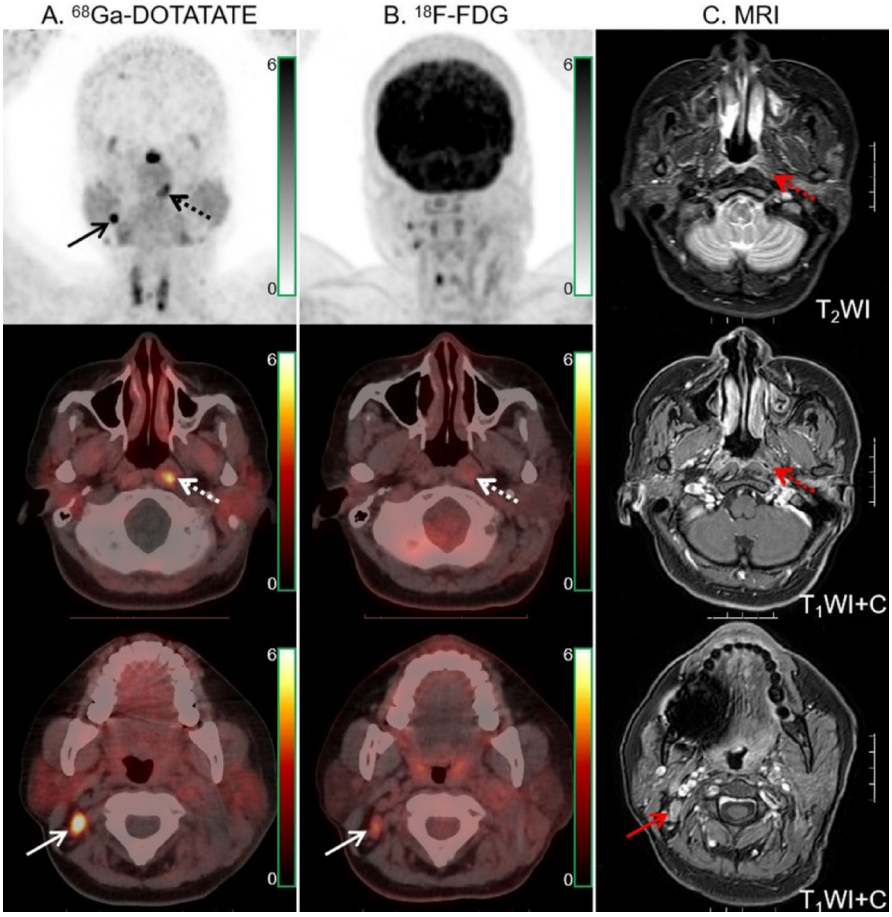

Fig. 1. ^{68}Ga-DOTATATE (**A**) and ^{18}F-FDG PET/CT (**B**) images in a 37-year-old woman with NPC. ^{68}Ga-DOTATATE PET/CT showed intensive tracer uptake in the primary tumor of the left pharyngeal recess (dotted arrow), while ^{18}F-FDG PET/CT and MRI (**C**) showed no abnormal findings in the corresponding region (dotted arrows). Moreover, ^{68}Ga-DOTATATE PET/CT revealed higher tracer uptake than ^{18}F-FDG PET/CT in the right cervical (level IIB) lymph node (solid arrows).

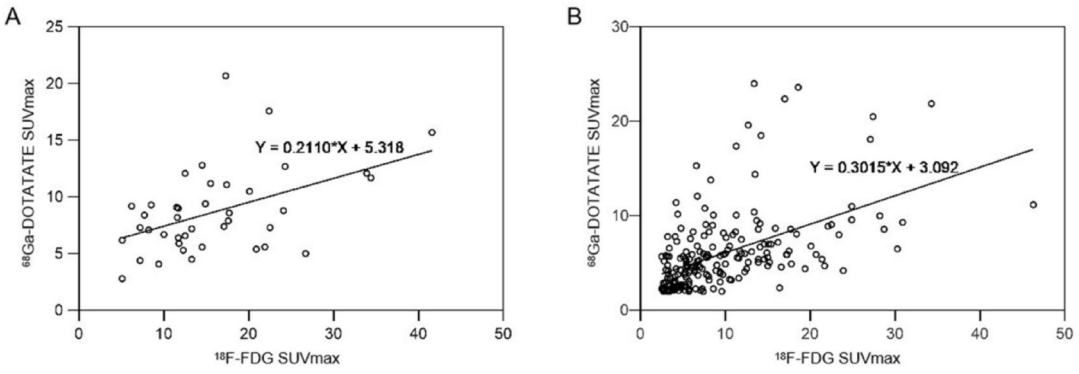

Fig. 2. Comparison of SUVmax of ^{68}Ga-DOTATATE and ^{18}F-FDG in matched double-positive primary tumors (A, $r = 0.466$, $p = 0.002$) and lymph nodes (B, $r = 0.51$, $p = 0.000$).

tumor recurrence showed no positive radiotracer uptake on ^{68}Ga-DOTATATE PET/CT ^{18}F-FDG uptake was significantly higher in primary tumors than in ^{68}Ga-DOTATATE. In 40 individuals, there was a moderate association between the two radiotracers' absorption by the primary tumor (Fig. 2A). MRI revealed 27 cases of invasion of the skull base bone and 11 occurrences of intracranial invasion. ^{68}Ga-DOTATATE PET/CT detected more skull base bone invasion (100% [27/27] vs. 96.3% [26/27]) and intracranial invasion (100% [11/11] vs. 54.5% [6/11]) than ^{18}F-FDG. Compared to ^{18}F-FDG, ^{68}Ga-DOTATATE PET/CT revealed a larger lesion area in

two invasions of the skull base bone and three intracranial invasions. The example in Fig. 3 demonstrated how the two approaches differed in determining primary tumor invasion.

Thirty-six of the forty-two people were suspected of having lymph node metastases. The assessment comprised 221 lymph nodes in total. Histopathology was employed as the reference standard for 27 lymph nodes, while morphological analysis and/or imaging follow-up were used to confirm the remaining lymph nodes. Finally, 202 lymph nodes were found to have metastasized, while the remaining 19 were classified as reactive hyperplastic or inflammatory lymph nodes. ^{68}Ga-DOTATATE PET/CT detection of lymph node metastases was comparable to ^{18}F-FDG PET/CT ^{18}F-FDG and ^{68}Ga-DOTATATE PET/CT revealed 18 and 4 false-positive lymph nodes, respectively ^{18}F-FDG uptake in lymph node metastases was greater than ^{68}Ga-DOTATATE. The absorption of both radiotracers by lymph node metastases was moderately correlated (Fig. 2B).

Of the forty-two people, six had visceral or bone metastases. ^{68}Ga-DOTATATE and ^{18}F-FDG PET/CT detected all 24 lung metastases. Compared to ^{18}F-FDG, ^{68}Ga-DOTATATE PET/CT showed more bone metastases; however, the difference was not statistically significant ($p = 0.07$). Compared to ^{18}F-FDG, ^{68}Ga-DOTATATE PET/CT displayed a decreased detection rate of liver metastases. ^{68}Ga-DOTATATE uptake was lower than ^{18}F-FDG in the lung and bone metastases when evaluating radiotracer uptake by distant metastases. However, liver metastases had higher uptake of ^{68}Ga-DOTATATE than ^{18}F-FDG. A sample patient with distant metastases is presented in Fig. 4.

Comparison of ^{68}Ga-DOTATATE PET/CT versus ^{18}F-FDG PET/CT for tumor staging

In seven cases, the T-stage was underestimated by ^{18}F-FDG PET/CT owing to the physiologically enhanced radiotracer uptake by normal brain tissue. The T-staging of one patient was underestimated due to the inability of ^{68}Ga-DOTATATE PET/CT to detect the return of the initial tumor. Furthermore, N-staging was overestimated by ^{18}F-FDG and ^{68}Ga-DOTATATE PET/CT in four and one patient, respectively. Moreover, in one case, the M-staging was underestimated by ^{18}F-FDG PET/CT and was rectified by ^{68}Ga-DOTATATE PET/CT.

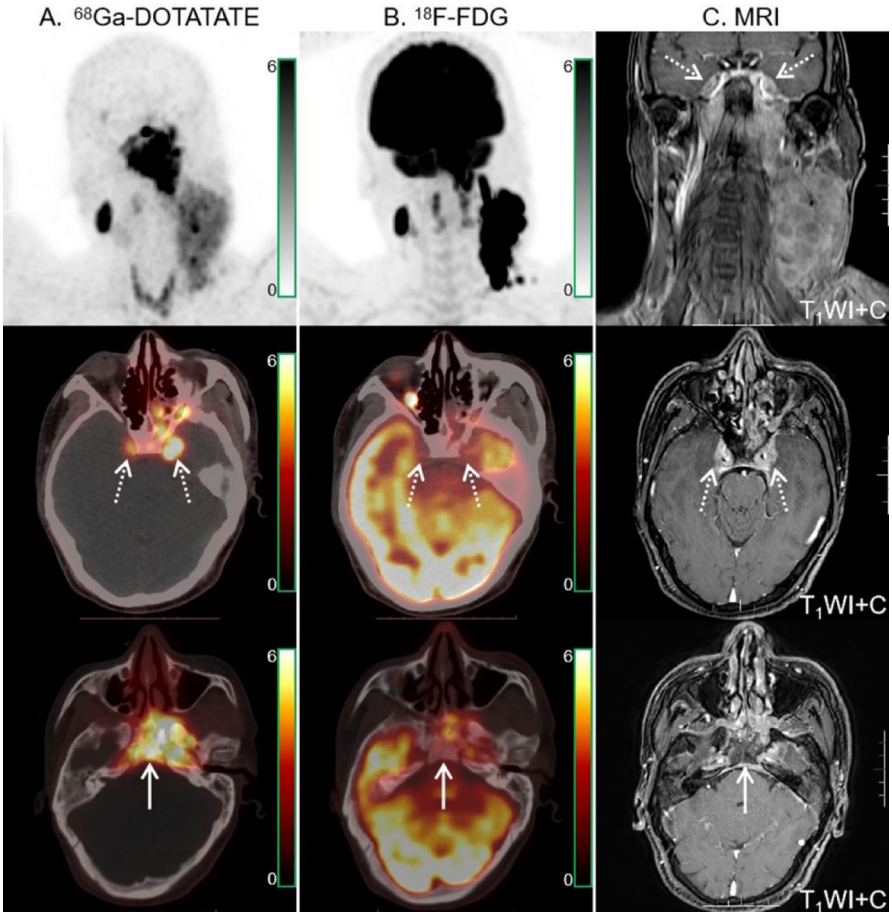

Fig. 3. ^{68}Ga-DOTATATE (**A**) and ^{18}F-FDG PET/CT (**B**) images in a 43-year-old man with NPC. Intense ^{68}Ga-DOTATATE uptake was observed in the bilateral cavernous sinuses (dotted arrows), suggesting intracranial invasion, but ^{18}F-FDG PET/CT revealed no abnormal intracranial ^{18}F-FDG uptake (dotted arrows). Moreover, ^{68}Ga-DOTATATE PET/CT showed strong tracer uptake in the sphenoid, occipital and petrous bones (solid arrow). The extent of skull base bone invasion (solid arrows) shown by ^{18}F-FDG PET/CT was significantly smaller than that shown by ^{68}Ga-DOTATATE PET/CT. MRI (**C**) findings were matched with ^{68}Ga-DOTATATE PET/CT.

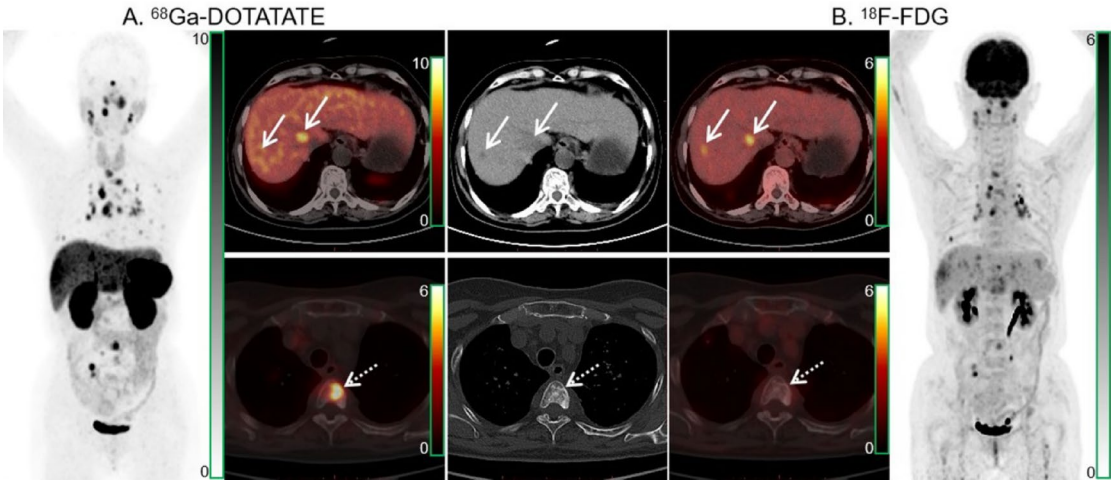

Fig. 4. ^{68}Ga-DOTATATE (**A**) and ^{18}F-FDG PET/CT (**B**) images in a 48-year-old woman with NPC. ^{68}Ga-DOTATATE and ^{18}F-FDG MIP images demonstrated multiple abnormal foci in the head, neck and trunk ^{18}F-FDG PET/CT showed more hepatic metastases than those shown in ^{68}Ga-DOTATATE PET/CT (solid arrows). The osteogenic metastasis (dotted arrows) revealed no significant ^{18}F-FDG uptake but intense ^{68}Ga-DOTATATE uptake.

Modalities and thresholds	Tumor volume (cm^3)	ICC	95% CI
MR + C	23.14 ± 21.61		
FDG—THbgd	16.91 ± 16.49	0.85	0.58–0.73
FDG—TH2.5	28.74 ± 26.22	0.88	0.73–0.94
FDG—TH40%	14.16 ± 10.61	0.63	0.25–0.82
TATE—THbgd	21.32 ± 19.72	0.95	0.91–0.99
TATE—TH2.5	19.08 ± 23.26	0.91	0.81–0.95
TATE—TH40%	19.37 ± 18.52	0.93	0.83–0.97

Table 3. Intra-group correlation analysis of the primary tumor volume measured by contrast-enhanced MR and ^{18}F-FDG PET/ ^{68}Ga-DOTATATE PET with different thresholds. *ICC* interclass correlation coefficient, *CI* confidence interval, *FDG* ^{18}F-FDG, *TATE* ^{68}Ga-DOTATATE.

Compared to ^{18}F-FDG, while ^{68}Ga-DOTATATE PET/CT resulted in inaccurate staging for one restaged patient, it correctly upstaged five patients (four from stage III to IVA and one from stage II to IVB) and correctly downstaged one patient (from stage III to II). Detailed clinical information and TNM staging for all patients are provided in the Supplementary Materials.

Comparison of primary tumor volume between ^{68}Ga-DOTATATE and ^{18}F-FDG PET/CT

Forty patients with primary tumors that could be detected were assessed. Tumor volumes and consistency analysis using various methods are displayed in Table 3. Tumor volume identified using various threshold techniques on ^{18}F-FDG PET/CT differed considerably. Compared to ^{18}F-FDG, ^{68}Ga-DOTATATE PET demonstrated reduced differences in tumor volume, aligning more closely with enhanced MRI findings. Tumor volume measured using THbgd thresholding in ^{68}Ga-DOTATATE PET was found to have the highest confidence and consistency with MRI (ICC: 0.95).

Discussion

This study demonstrated that ^{68}Ga-DOTATATE and ^{18}F-FDG PET/CT have comparable performance in the detection of primary tumors and lymph node metastases. ^{68}Ga-DOTATATE PET/CT demonstrated an equivalent number of lung metastases, revealing a greater number of bone metastases than ^{18}F-FDG PET/CT. However, ^{68}Ga-DOTATATE PET/CT was unable to detect liver metastases accurately. In 35/42 patients, ^{68}Ga-DOTATATE and ^{18}F-FDG PET/CT yielded consistent overall staging. In 6/42 patients, the overall staging on ^{18}F-FDG PET/CT was corrected using ^{68}Ga-DOTATATE PET/CT. Furthermore, tumor volumes defined by 68Ga-DOTATATE PET using various thresholds demonstrated greater concordance with MRI than ^{18}F-FDG PET. As a result, ^{68}Ga-DOTATATE PET/CT demonstrates significant clinical potential as an innovative imaging technique for evaluating NPC.

Compared to previous results[14], this study demonstrated that primary tumors and lymph node metastases showed significantly higher uptake of ^{18}F-FDG than ^{68}Ga-DOTATATE. This may result from variations among

the distinct small study cohorts. The uptake of the two radiotracers demonstrated a strong correlation despite differing imaging principles in paired double-positive primary tumors and lymph node metastases. The metabolic activity of a tumor serves as an indicator of its aggressiveness. The aggressiveness of certain cancers is positively correlated with SSTR expression[22,23]. This suggests that ^{68}Ga-DOTATATE imaging could be useful in predicting the aggressiveness of NPC. In one of thirty-seven newly diagnosed patients, the uptake of ^{68}Ga-DOTATATE was significant. However, MRI and ^{18}F-FDG PET/CT could not identify the primary tumor. This suggests that ^{68}Ga-DOTATATE PET/CT may demonstrate improved efficacy in identifying early mucosal lesions compared to traditional techniques. The efficacy of ^{18}F-FDG PET/CT in distinguishing localized residual or recurrent disease from inflammation following NPC radiotherapy remains a subject of debate[24]. However, ^{68}Ga-DOTATATE PET/CT was not more accurate than ^{18}F-FDG imaging in the relapsed cases. The limited number of relapsed cases necessitates further investigation into detecting localized recurrence of NPC using ^{68}Ga-DOTATATE PET/CT ^{18}F-FDG, as a nonspecific tumor radiotracer, shows significant uptake in inflammatory lesions[4]. In this study, 18 lymph nodes with inflammatory or reactive hyperplasia displayed aberrant ^{18}F-FDG uptake, whereas only 4 were false-positive on ^{68}Ga-DOTATATE PET/CT. The N-staging of four patients was revised using ^{68}Ga-DOTATATE PET/CT. Therefore, ^{68}Ga-DOTATATE PET/CT may have higher specificity than ^{18}F-FDG PET/CT in detecting lymph node metastases in patients with nasopharyngeal carcinoma.

In assessing distant metastases, lung, and bone metastases demonstrated a higher absorption of ^{18}F-FDG compared to ^{68}Ga-DOTATATE, whereas liver metastases demonstrated the inverse trend. The limitation of ^{68}Ga-DOTATATE PET in identifying liver metastases arises from its inability to detect lesions with tracer uptake comparable to that of normal liver tissue, where SSTR2 expression is significantly elevated, thus decreasing the detection rate of liver metastases. ^{68}Ga-DOTATATE PET/CT detected more bone metastases than ^{18}F-FDG PET/CT. However, one bone metastasis (bone abnormality not shown on CT) was not detected by ^{68}Ga-DOTATATE PET/CT, suggesting that it may not be sufficiently sensitive for detecting early bone metastases compared with ^{18}F-FDG PET/CT ^{18}F-FDG PET/CT was not sensitive enough to identify osteogenic metastases[25]. This study found that bone metastases lacking ^{18}F-FDG positive uptake showed osteosclerosis on CT imaging. All demonstrated positive radiotracer uptake on ^{68}Ga-DOTATATE PET/CT. One patient experienced a benefit from 68Ga-DOTATATE PET/CT, which corrected the M-staging of ^{18}F-FDG, leading to appropriate treatment. While ^{68}Ga-DOTATATE PET/CT showed high accuracy in identifying osteoblastic metastases of NPC in our study, cases of false-positive results were observed under specific conditions. Uptake of ^{68}Ga-DOTATATE is observable in osteoblastic bone diseases due to the expression of somatostatin receptor type 2 by osteoblasts[26]. Degenerative bone disease, fractures, fibrous dysplasia, and vertebral hemangiomas all show ^{68}Ga-DOTATATE uptake[27–29]. Integration with other imaging findings, such as CT/MRI characteristics and clinical data during imaging, is essential for differentiating between benign and malignant lesions rather than relying solely on ^{68}Ga-DOTATATE uptake levels.

The precise measurement of tumor volume is essential for effective radiotherapy planning. The significant absorption of ^{18}F-FDG by adjacent normal tissue complicates the evaluation of tumor extent using ^{18}F-FDG PET/CT[30]. The lack of a unified segmentation method for lesions and the selection of SUV thresholds also led to low credibility in tumor volume delineated by ^{18}F-FDG PET[31]. The study demonstrated that ^{68}Ga-DOTATATE PET/CT exceeded ^{18}F-FDG in assessing skull base bone, intracranial invasion, and T staging. This occurs due to the limited absorption of ^{68}Ga-DOTATATE by the normal tissues surrounding the head and neck. This also functions as a prerequisite for precisely defining the biological target area in radiotherapy. In this study, the tumor volume measured by alternative threshold techniques was less than that obtained from MRI, except for ^{18}F-FDG PET using TH2.5. This may result from interference caused by peritumoral edema and inflammation, which can lead to an overestimation of the tumor's extent on MRI[32]. The tumor volume segmented using TH2.5 on ^{18}F-FDG PET is relatively large. This is mainly because it is difficult to fully distinguish the boundary between the primary tumor and the adjacent non-tumor tissues with this threshold method. Compared with ^{18}F-FDG PET, the tumor volumes measured by these three thresholds on ^{68}Ga-DOTATATE PET showed smaller changes and were more consistent with MRI. The application of THbgd as a threshold method on ^{68}Ga-DOTATATE PET for tumor volume assessment demonstrated the highest consistency with MRI results. Previous studies indicate that the THbgd exceeds other fixed threshold methods in tumor volume delineation[21,33,34]. The investigators observed that the ^{18}F-FDG PET/CT using THbgd demonstrated a significantly higher detection rate of recurrent and metastatic lesions than TH2.5 and TH40%[21]. Therefore, it was speculated that ^{68}Ga-DOTATATE PET/CT is a reliable supplement to MRI for helping with tumor volume delineation in NPC. Recently, Beichel et al.[35] demonstrated advantages in ^{18}F-FDG PET scans of head and neck tumors using a highly automated optimal surface segmentation method for uptake volume segmentation. This semiautomated segmentation approach, which integrates graph-based optimization with the just-enough-interaction principle, can adapt to metabolic characteristics of different tracers and has the potential to be further explored as a lesion segmentation method for ^{68}Ga-DOTATATE PET scans in the future.

The limited number of participants represents a significant limitation of this study. Larger population sizes are required for prospective studies. This study employed multimodality imaging and follow-up examinations to identify most metastases, as collecting histopathologic results for all metastases was not clinically feasible. Therefore, further pathological evidence of metastases is required to confirm the diagnostic accuracy of ^{68}Ga-DOTATATE PET/CT. Furthermore, visual bias affects tumor volumes on MRI, which are defined by visual assessment. In the future, it is necessary to enhance the study methodology to provide a more detailed analysis of the efficacy of ^{68}Ga-DOTATATE PET/CT in NPC.

Conclusion

In conclusion, the ^{68}Ga-DOTATATE PET/CT exhibited great clinical utility in evaluating NPC diagnosis and staging. In identifying bone metastases, lymph node metastases, skull base invasion, and intracranial involvement,

^{68}Ga-DOTATATE PET/CT may demonstrate improved efficacy compared to ^{18}F-FDG. The ^{68}Ga-DOTATATE PET/CT can obtain accurate tumor volume delineation. *Using THbgd as the ideal threshold technique could be a valuable addition to MRI for NPC target volume delineation. Further research is necessary to determine the clinical usefulness of ^{68}Ga-DOTATATE PET/CT in radiotherapy planning for NPC.*

Data availability

The data that support the findings of this study are available from the corresponding author upon reasonable request.

Received: 15 February 2025; Accepted: 29 April 2025
Published online: 09 May 2025

References

1. Chen, Y. P. et al. Nasopharyngeal carcinoma. *Lancet* **394**, 64–80 (2019).
2. Sung, H. et al. Global cancer statistics 2020: GLOBOCAN estimates of incidence and mortality worldwide for 36 cancers in 185 countries. *CA Cancer J. Clin.* **71**, 209–249 (2021).
3. Au, K. H. et al. Treatment outcomes of nasopharyngeal carcinoma in modern era after intensity modulated radiotherapy (IMRT) in Hong Kong: A report of 3328 patients (HKNPCSG 1301 study). *Oral Oncol.* **77**, 16–21 (2018).
4. Lee, S. H. et al. Diagnostic value of only ^{18}F-fluorodeocyglucose positron emission tomography/computed tomography-positive lymph nodes in head and neck squamous cell carcinoma. *Otolaryngol. Head Neck Surg.* **147**, 692–698 (2012).
5. Fei, Z. et al. Metabolic tumor volume and conformal radiotherapy based on prognostic PET/CT for treatment of nasopharyngeal carcinoma. *Medicine* **98**, e16327 (2019).
6. van den Bosch, S. et al. 18)F-FDG-PET/CT-based treatment planning for definitive (chemo)radiotherapy in patients with head and neck squamous cell carcinoma improves regional control and survival. *Radiother Oncol.* **142**, 107–114 (2020).
7. Zaidi, H. & El Naqa, I. PET-guided delineation of radiation therapy treatment volumes: a survey of image segmentation techniques. *Eur. J. Nucl. Med. Mol. Imaging*. **37**, 2165–2187 (2010).
8. Riegel, A. C. et al. Variability of gross tumor volume delineation in head-and-neck cancer using CT and PET/CT fusion. *Int. J. Radiat. Oncol. Biol. Phys.* **65**, 726–732 (2006).
9. Hong, R., Halama, J., Bova, D., Sethi, A. & Emami, B. Correlation of PET standard uptake value and CT window-level thresholds for target delineation in CT-based radiation treatment planning. *Int. J. Radiat. Oncol. Biol. Phys.* **67**, 720–726 (2007).
10. Heron, D. E. et al. Hybrid PET-CT simulation for radiation treatment planning in head-and-neck cancers: a brief technical report. *Int. J. Radiat. Oncol. Biol. Phys.* **60**, 1419–1424 (2004).
11. Xu, M. et al. Genome sequencing analysis identifies Epstein-Barr virus subtypes associated with high risk of nasopharyngeal carcinoma. *Nat. Genet.* **51**, 1131–1136 (2019).
12. Lechner, M. et al. Somatostatin receptor 2 expression in nasopharyngeal cancer is induced by epstein barr virus infection: impact on prognosis, imaging and therapy. *Nat. Commun.* **12**, 117 (2021).
13. Viswanathan, K. & Sadow, P. M. Somatostatin receptor 2 is highly sensitive and specific for Epstein-Barr virus-associated nasopharyngeal carcinoma. *Hum. Pathol.* **117**, 88–100 (2021).
14. Zhao, L. et al. Somatostatin receptor imaging with [(68)Ga]Ga-DOTATATE positron emission tomography/computed tomography (PET/CT) in patients with nasopharyngeal carcinoma. *Eur. J. Nucl. Med. Mol. Imaging*. **49**, 1360–1373 (2022).
15. Zheng, J. et al. A head-to-head comparison of [(68)Ga]Ga-DOTATATE and [(68)Ga]Ga-FAPI PET/CT in patients with nasopharyngeal carcinoma: a single-center, prospective study. *Eur. J. Nucl. Med. Mol. Imaging*. **51**, 3472–3474 (2024).
16. Liu, L. et al. The impact of total variation regularized expectation maximization reconstruction on (68)Ga-DOTA-TATE PET/CT images in patients with neuroendocrine tumor. *Front. Med. (Lausanne)*. **9**, 845806 (2022).
17. Ding, H. et al. Prospective comparison of (68)Ga-FAPI-04 and (18)F-FDG PET/CT for tumor staging in nasopharyngeal carcinoma. *Front. Oncol.* **12**, 1047010 (2022).
18. Pan, J. J. et al. Ninth version of the AJCC and UICC nasopharyngeal cancer TNM staging classification. *JAMA Oncol.* **10**, 1627–1635 (2024).
19. Caudell, J. J. et al. NCCN guidelines® insights: head and neck cancers, version 1.2022. *J. Natl. Compr. Cancer Netw.* **20**, 224–234 (2022).
20. Eisenhauer, E. A. et al. New response evaluation criteria in solid tumours: revised RECIST guideline (version 1.1). *Eur. J. Cancer*. **45**, 228–247 (2009).
21. Tian, Y. et al. Prognostic value of volume-based positron emission tomography/computed tomography in nasopharyngeal carcinoma patients after comprehensive therapy. *Contrast Media Mol. Imaging* **2018**, 1384281 (2018).
22. Provost, C. et al. ^{68}Ga-DOTATOC and FDG PET imaging of preclinical neuroblastoma models. *Anticancer Res.* **36**, 4459–4466 (2016).
23. de Sá, S. V. et al. Somatostatin receptor subtype 5 (SSTR5) mRNA expression is related to histopathological features of cell proliferation in insulinomas. *Endocr. Relat. Cancer*. **13**, 69–78 (2006).
24. OuYang, P. Y. et al. Benefit of [(18)F] FDG PET/CT in the diagnosis and salvage treatment of recurrent nasopharyngeal carcinoma. *Eur. J. Nucl. Med. Mol. Imaging*. **50**, 881–891 (2023).
25. Zhang, Y. et al. Comparison of (18)F-NaF PET/CT and (18)F-FDG PET/CT for detection of skull-base invasion and osseous metastases in nasopharyngeal carcinoma. *Contrast Media Mol. Imaging* **2018**, 8271313 (2018).
26. Mackie, E. J., Trechsel, U. & Bruns, C. Somatostatin receptors are restricted to a subpopulation of osteoblast-like cells during endochondral bone formation. *Development* **110**, 1233–1239 (1990).
27. Klinaki, I., Al-Nahhas, A., Soneji, N. & Win, Z. ^{68}Ga DOTATATE PET/CT uptake in spinal lesions and MRI correlation on a patient with neuroendocrine tumor: potential pitfalls. *Clin. Nucl. Med.* **38**, e449–453 (2013).
28. Filizoglu, N., Bugdayci, O. & Ozguven, S. Sacral insufficiency fracture on ^{68}Ga-DOTATATE PET/CT. *Clin. Nucl. Med.* **46**, e490–e491 (2021).
29. Papadakis, G. Z. et al. Fibrous dysplasia mimicking malignancy on ^{68}Ga-DOTATATE PET/CT. *Clin. Nucl. Med.* **42**, 209–210 (2017).
30. King, A. D. et al. The impact of ^{18}F-FDG PET/CT on assessment of nasopharyngeal carcinoma at diagnosis. *Br. J. Radiol.* **81**, 291–298 (2008).
31. Chen, Y. Z. et al. Evaluation of time-phase effect on ^{18}F-FDG PET/CT delineation methods for treatment planning of nasopharyngeal carcinoma. *Clin. Nucl. Med.* **41**, 354–361 (2016).
32. Ng, S. H. et al. Clinical usefulness of ^{18}F-FDG PET in nasopharyngeal carcinoma patients with questionable MRI findings for recurrence. *J. Nucl. Med.* **45**, 1669–1676 (2004).
33. Yu, W. et al. Y. GTV Spatial conformity between different delineation methods by ^{18}FDG PET/CT and pathology in esophageal cancer. *Radiother Oncol.* **93**, 441–446 (2009).

34. Li, C. et al. Evaluation of ^{11}C-choline PET/CT for T staging and tumor volume delineation in nasopharyngeal cancer patients in comparison to ^{18}F-FDG PET/CT. *Clin. Nucl. Med.* **48**, 563–573 (2023).
35. Beichel, R. R. et al. Semiautomated segmentation of head and neck cancers in ^{18}F-FDG PET scans: A just-enough-interaction approach. *Med. Phys.* **43**, 2948–2964 (2016).

Acknowledgements
The authors are grateful to the members of Department of Nuclear Medicine, The Affiliated Hospital, Southwest Medical University and Nuclear Medicine and Molecular Imaging Key Laboratory of Sichuan Province for their technical guidance, cooperation and assistance in completing this article.

Author contributions
All authors contributed to the study conception and design. Material preparation, data collection and analysis were performed by H.Y.D. and L.J. The first draft of the manuscript was written by H.Y.D. and all authors commented on previous versions of the manuscript. All authors read and approved the final manuscript.

Funding
This work was supported by Luzhou Science and Technology Program (2024JYJ054), National Natural Science Foundation of China (U20A20384), Health Commission of Sichuan Province (21ZD005), Science and Technology Major Project of Gansu Province (23ZDFA014), and Isotope and Drug Innovation Fund of National Engineering Research Center for Isotopes and Drugs (TWSCX-2023-CXJJ-3-1).

Declarations

Competing interests
The authors declare no competing interests.

Ethical approval
This study was approved by the Institutional Review Board of the Affiliated Hospital of Southwest Medical University (2020035). All procedures involving human participants were performed in accordance with the ethical standards of the institutional committee, as well as the 1964 Helsinki Declaration and its later amendments or comparable ethical standards. This study does not contain any animal experiments. Informed consent was obtained from all participants included in the study.

Additional information
Supplementary Information The online version contains supplementary material available at https://doi.org/10.1038/s41598-025-00625-y.

Correspondence and requests for materials should be addressed to Y.L. or Y.C.